Bioresource Technology 258 (2018) 142–150

Contents lists available at ScienceDirect

Bioresource Technology

journal homepage: www.elsevier.com/locate/biortech

Evaluation of process performance, energy consumption and microbiota characterization in a ceramic membrane bioreactor for ex-situ biomethanation of H_2 and CO_2

Natalia Alfaro, María Fdz-Polanco, Fernando Fdz-Polanco, Israel Díaz*

Department of Chemical Engineering and Environmental Technology, Escuela de Ingenierías Industriales, Sede Dr. Mergelina, University of Valladolid, Dr. Mergelina s/n, 47011 Valladolid, Spain

GRAPHICAL ABSTRACT

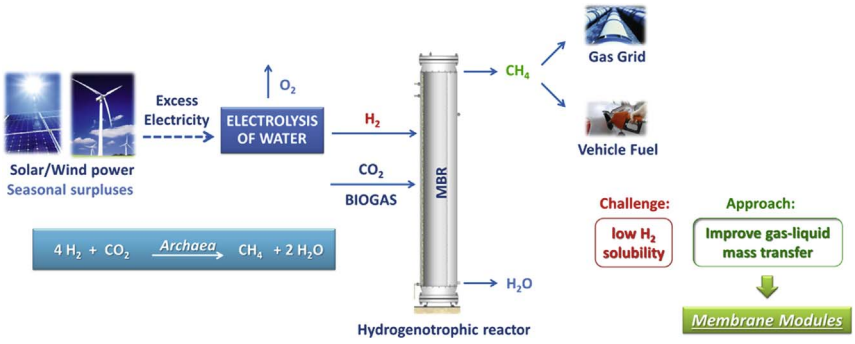

ARTICLE INFO

Keywords:
Ex-situ upgrading
Biomethane
MBR
Hydrogenotrophic *archaea*
Methanation

ABSTRACT

The performance of a pilot ceramic membrane bioreactor for the bioconversion of H_2 and CO_2 to bioCH_4 was evaluated in thermophilic conditions. The loading rate was between 10 and 30 $m^3\ H_2/m^3_{reactor}\ d$ and the system transformed 95% of H_2 fed. The highest methane yield found was 0.22 $m^3\ CH_4/m^3\ H_2$, close to the maximum stoichiometric value (0.25 $m^3\ CH_4/m^3\ H_2$) thus indicating that *archaeas* employed almost all H_2 transferred to produce CH_4. k_La value of 268 h^{-1} was reached at 30 $m^3\ H_2/m^3_{reactor}\ d$. DGGE and FISH revealed a remarkable *archaeas* increase related to the selection-effect of H_2 on community composition over time. *Methanothermobacter thermautotrophicus* was the *archaea* found with high level of similarity. This study verified the successful application of membrane technology to efficiently transfer H_2 from gas to the liquid phase, the development of a hydrogenotrophic community from a conventional thermophilic sludge and the technical feasibility of the bioconversion.

1. Introduction

The production of biomethane is gaining attention within the countries of the European Union, because of two reasons; firstly, it allows to reduce reliance on natural gas imports (EurObserver, 2014) and secondly, permiting its transport and utilization far from the place where it is obtained. In this context, the bioconversion of H_2 and CO_2 to biomethane by means of methanogenic *archaea* according to reaction

$$4H_2 + CO_2 \rightarrow CH_4 + 2H_2O \quad (1)$$

* Corresponding author.
E-mail address: israel.diaz@iq.uva.es (I. Díaz).

https://doi.org/10.1016/j.biortech.2018.02.087
Received 28 December 2017; Received in revised form 16 February 2018; Accepted 17 February 2018
Available online 23 February 2018
0960-8524/

has an important economic, environmental and energetic interest; specially in the actual context of renewable energies implementation because the bioconversion of CO_2 (or biogas) into biomethane can create a synergy between renewable energies. On the one side, H_2 generation from water electrolysis from wind and solar power can be the solution of the variable wind power production, site-specificity of this source and electricity storage (Levene et al., 2007; Ni et al., 2006). EU countries with high implementation of renewable energies, suffer of seasonal surpluses where production exceeds demand and an appreciable portion of electricity production is lost in most cases. H_2 obtained from water electrolysis from excess electricity production from wind and solar power allows long-term energy storage and avoids energy squandering (Cruz, 2008), which is an important and remarkable point nowadays in the idea of environmental conservation and responsible use of energy. However, H_2 limitations and drawbacks are linked to its transportation and management (Granovskii et al., 2006) because of its low density which requires high storage volumes and the technology for direct utilization is not developed yet. Then, the direct transformation of H_2 into biomethane by coupling it with CO_2/biogas permits renewable energy in the form of biomethane to be stored, injected and distributed through the natural gas grid or employed as fuel for vehicles (Deublein and Steinhauser, 2011; Deng and Hägg, 2010). Additionally, anaerobic digestion of biomass, organic wastes and by-products is an effective and well-established renewable energy technology for bioenergy production in the EU (EurObservER, 2013) which produces a biogas with a typical content of 30–40% CO_2 and 70–60% CH_4. This biogas can be upgraded by means of hydrogenotrophic *archaeas* and an external source of H_2 from water electrolysis from surplus wind and solar power (according to Eq. (1) and then, the rate of biomethane increased, increasing its heating value and its potential applications as alternative to natural gas (Deng and Hägg, 2010). At the same time, this technology fixs CO_2 by means of its chemoautotrophic conversion with H_2 to biomethane, decreasing the CO_2 emissions to the atmosphere and then the greenhouse gases, reducing by this way its impact in the global warming which can be translated into an effective CO_2 mitigation technology. Biomethane production from the synergy between the above mentioned renewable energies is a promising and effective method for bioenergy production. Commercial technologies (as PSA, membrane separation, scrubbing, absorption, cryogenic separation or chemical treatment) only separate CH_4 from CO_2 thus requiring further steps to avoid CO_2 emissions, the use of chemical substances, high pressures and temperatures and energy input increasing process costs (Bauer et al., 2013; Luo and Angelidaki, 2012). However, biological biogas upgrading constitutes a cheaper and environmentally friendly alternative technology moving towards sustainable energy production.

Two different approaches are shown in literature in order to remove CO_2 by hydrogenotrophic methanogenesis. The first approach is the addition of H_2 to conventional anaerobic digesters of organic matter with the aim of removing CO_2 from biogas while increasing the production of biomethane named in-situ biogas upgrading (Luo et al., 2012; Wang et al., 2013; Luo and Angelidaki, 2013; Bassani et al., 2016). The second is ex-situ biogas upgrading, the supply of H_2 and CO_2 (or biogas) to an exclusively methanogenic bioreactor rich in methanogenic *archaeas* (Burkhardt and Busch, 2013; Kim et al., 2013; Lee et al., 2012; Luo and Angelidaki, 2012; Ju et al., 2008; Peillex et al., 1990; Kougias et al., 2017; Bassani et al., 2017; Bassani et al., 2015).

The gas-liquid mass transfer of H_2 was found to be the main constraint to the successful development of the technology in both approaches due to its low solubility (dimensionless Henry's constant = 55 $g/L_G/g/L_{H2O}$ at 55 °C). Different methods of gas-liquid mass transfer of H_2 have been performed up to now. Gas diffusers on lab-scale CSTR were shown to require high stirring speed employing a pure culture of *Methanobacterium thermoautotrophicum* at 65 °C (Peillex et al. 1990) or mixed methanogens cultures at thermophilic conditions (55 °C) (Luo and Angelidaki, 2012; Bassani et al., 2015). Lab-scale packed columns bioreactors at mesophilic conditions (35 °C) with a mixed culture were studied as well (Lee et al., 2012). Moreover, up-flow reactors were experienced in lab-scale (Kougias et al., 2017; Bassani et al., 2017). Membrane bioreactors (MBR) were also evaluated for the transfer of H_2 by gas diffusion through the membrane material (Díaz et al., 2015; Strevett et al., 1995; Wang et al., 2013; Ju et al., 2008; Bassani et al., 2016). Scant literature of reactors with volume higher than 10 L has been found: Burkhardt and Busch (2013) used a trickled-bed bioreactor in a 26.8 L of reactor working volume at 35 °C; Kim et al. (2013) studied in a 100 L CSTR at moderate stirring speed at mesophilic conditions and Díaz et al. (2015) performed the biogas upgrading in a membrane bioreactor of 31 L working volume at 55 °C using a polymeric membrane as gas-liquid mass transfer method.

Polymeric membranes as the hollow-fiber experienced previously have a temperature work range up to 40 °C (Suez Water Technologies – GE, 2014) so in a long-term they can produce operating problems being damaged on account of thermophilic conditions. However, ceramic membrane modules are able to work with high temperatures up to 90 °C (Atech Innovations, 2014). Therefore, from an industrial point of view, the working temperature challenge present in polymeric membranes can be solved with the use of ceramic MBRs allowing the biological conversion to take place satisfactorily in a long-term. The utilization of a ceramic membrane bioreactor (MBR) to convert H_2 and CO_2 to bioCH_4 in thermophilic conditions to overcome the limitations to mass transfer of H_2 and the long-term operability was evaluated in this study. In addition, higher scale than which was used in previous studies of literature was experienced moving towards industrial scale. The ceramic membrane module was employed to create a large gas sparging surface and the feasibility of the technology was assessed.

2. Materials and methods

2.1. Pilot plant

The experiment was performed using one insulated cylindrical membrane bioreactor with a working volume of 60 L in which an electric resistance was used to heat reactor walls. Reactor was equipped with a ceramic tubular membrane module (ATECH, Germany) consisted of 28 tubes of Al_2O_3 with 0.8 μm pore size and an area of approximately 1 m^2 which was used as gas sparging surface in order to generate fine small bubbles. Hydrogenotrophic reactor was fed continuously with H_2 and CO_2 from gas cylinders and two mass-flow controllers (Aalborg, USA) were used to regulate the rate of both gases. Feed and recirculation lines were mixed and then preheated in a thermostatic bath at 55 °C. The gas mixture was injected in the reactor through upper part of ceramic membrane as given in schematic representation of the reactor in Fig. 1. The reactor counted with a compressor to recirculate biogas from the reactoŕs headspace through the membrane module. A peristaltic pump was employed to avoid solids deposition at a rate of 1000 mL/min.

2.2. Operating conditions

Anaerobic sludge from a thermophilic anaerobic digester at the laboratory treating activated sludge from the WWTP of Valladolid (Spain) was used to inoculate the reactor in a total amount of 60 L. A set-up period was performed at thermophilic conditions by supplying H_2 and CO_2 in a ratio of 4:1 (according to the stoichiometric values of Eq. (1) at a loading rate (LR) of 5.0 $m^3H_2/m^3_{reactor}$ d with a gas recirculation rate (Q_R) of 11.6 m^3/d for 30 days (all values expressed at 55 °C and 1 atm). Afterwards, the experiment started maintaining thermophilic conditions in which a range between 10 and 30 $m^3H_2/m^3_{reactor}$ d was studied in four stages according to Table 1 with the objective of determining the maximum LR that could be applied with a 95% conversion efficiency for methane. In order to evaluate reactor performance and mass transfer conditions different recirculation rates were applied in some stages. Nutrients required for microbial activity and a phosphate buffer

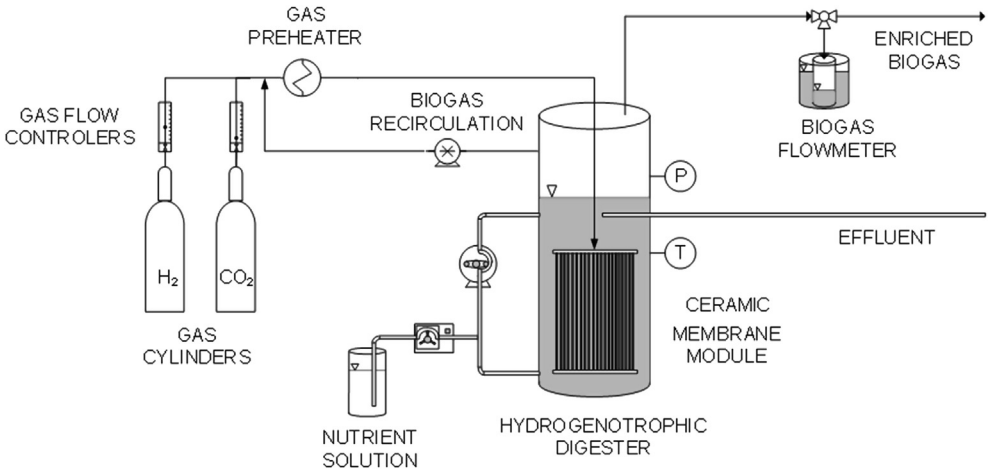

Fig. 1. Diagram of the MBR studied in the experiment.

Table 1
Operating conditions studied during the experiment.

	Stage 1	Stage 2		Stage 3
		2a	2b	
t (d)	0	26	86	137
LR ($m^3H_2/m^3_{reactor}$ d)	10	20	20	30
Q_R (L/min)	8.0	8.0	12.3	12.3

solution were supplied when the concentration of NH_4^+ and PO_4^{3-} fell below 500 mg/L as in Díaz et al., 2015, macronutrients and micronutrients were added too. The macronutrient solution was prepared like the stock solution A reported in Angelidaki and Sanders (2004), while the micronutrients solution was a version that was modified (by adding 500 mg/L of resazurine) from the trace-metal solution also from Angelidaki and Sanders (2004). Both solutions were used during the set-up period and stages 1-2a every 20 days approximately and the centrate wastewater from the centrifugation of anaerobically digested mixed sludge of the wastewater treatment plant of Valladolid (Spain) was used as nutrient solution during stages 2b-3 at a flow of 143 mL/day with a HRT of 420 days. The phosphate buffer solution was prepared with $K_2HPO_4{\cdot}3H_2O$ and KH_2PO_4 to a final pH of 7.4 like in Díaz et al. (2015).

2.3. Monitoring and analysis

Temperature was maintained at 55 ± 1 °C during the experiment and was controlled with a PID and a PT100 probe. For this purpose the walls of the insulated reactor were heated with an electric resistance. Headspace pressure was monitored with an Endress Hauser Cerabar PMC131 probe. A gas flowmeter was employed to measure the effluent gas rate by liquid displacement and the composition of the obtained biogas (dry basis) was determined by gas chromatography (GC-TCD) as described in Díaz et al. (2010) on a daily basis using gas sample point to obtain the biogas sample. A graduate cylinder was used to collect liquid effluent daily. pH, total suspended solids (TSS), volatile suspended solids (VSS), total solids (TS), volatile solids (VS) and NH_4^+ values were analyzed on a week basis according to Standard Methods (APHA, 2005). VFA concentration was analyzed weekly by gas chromatography (GC-FID) following the method reported in Díaz et al. (2010). Liquid sample was collected in liquid sample point in order to obtain above physicochemical parameters.

2.4. Calculations

Calculations about efficiency of H_2 utilization, methane yield, mass flow rate of H_2 transferred from gas to liquid phase, effluent mass flow rate of CH_4 gas as equivalent H_2, k_La_{H2} and k_La_{CO2} values, maximum specific utilization rate and fraction of H_2 employed for methanogen growth have been performed following calculations in Díaz et al. (2015). CH_4 and H_2 in the liquid effluent can be neglected due to the low solubility of CH_4 in water (Adimensional Henrýs constant is 43 at 55 °C) and H_2 is several orders of magnitude lower than the H_2 mass flow rates in gaseous streams. In steady state conditions, assuming all the resistance to mass transfer is in the gas/liquid interphase, mass flow rate of H_2 transferred from gas to liquid phase was calculated. H_2 concentration in the liquid phase is negligible as a result of H_2 complete consumption by methanogens in this phase.

To calculate the energy consumption of the system when upgrading biogas (CH_4/CO_2, 60/40 %v.), a steady-state energy balance was performed according to the scheme shown in Fig. 2. The reference state is chosen to be $T_0 = 25$ °C and $P_0 = 1$ atm. The power (kW) required for gas compression (W_1 *and* W_2) was determined with Eq. (2) (Perry et al., 1999):

$$W = 2.78{\cdot}10^{-4}\dot{V}\,P_1 \ln\frac{P_2}{P_1} \tag{2}$$

where $\dot{V}$ is the volumetric flowrate of the stream (m^3/s) and P_1 and P_2

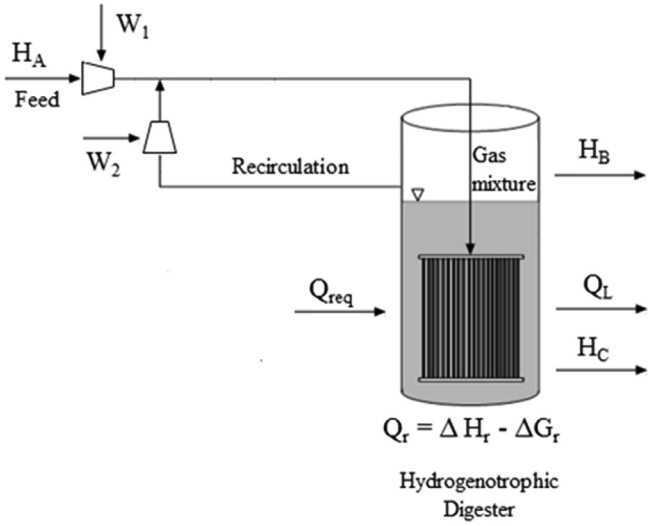

Fig. 2. Diagram of energy streams.

the absolute inlet pressure and absolute discharge pressure (kPa) respectively.

H_i (kW), the specific enthalpy of the stream i, is given by Eq. (3):

$$H_i = \dot{m}_l \cdot C_{p_i}(T_i - T_0) \quad (3)$$

where $\dot{m}_l$ is the mass flow rate (kg/s) of stream i, C_{p_i} the specific heat (kJ/kg K) of stream i, and *Ti* the temperature (K) of the stream. The values of C_p for the substances involved are 14.3, 0.8, 2.2, 2.08 and 4.184 kJ/kg K for H_2, CO_2, CH_4, H_2O vapor and H_2O liquid correspondingly (NIST Chemistry WebBook, NIST Standard Reference Database Number 69).

Heat losses in the vessel (Q_L) are defined by Eq. (4):

$$Q_L = UA(T_{IN} - T_{OUT}) \quad (4)$$

where U is the global heat transfer coefficient ($0.5 \cdot 10^{-3}$ kW/m^2 K), A the specific heat transfer surface (m^2) considering a 10 m length column (the diameter was adjusted to mass flow rate to fit a loading rate of 30 $m^3H_2/m^3_{reactor}$ d), T_{IN} the temperature inside the vessel (328 K) and T_{OUT} the minimum ambient temperature (273 K).

The heat rate (kW) released by the biological reaction was approximated by Eq. (5), assuming that free enthalpy (ΔG_R^0) is the amount of enthalpy that can be employed by microorganisms (Madigan and Brock, 2009):

$$Qr = 0.88\frac{n_{H2}}{4}(\Delta H_R^0 - \Delta G_R^0) \quad (5)$$

where 0.88 is the efficiency of substrate conversion to CH_4, n'_{H2} is molar flow rate of H_2 supplied (mol/s), 4 the stoichiometric coefficient for H_2 in Eq. (1), and ΔH_R^0 and ΔG_R^0 the enthalpy and Gibbs free energy variations in Eq. (1), −165.0 and −113.6 kJ/mol correspondingly.

Then, the total energy consumption (kW) of the system shown in Fig. 2 can be calculated as (Eq. (6):

$$Total\ Energy\ Consumption = (H_A + H_B + H_C + Q_L + Q_r) + (W_1 + W_2) \quad (6)$$

where the terms within the first parenthesis correspond to enthalpy/heat rates and W_1 and W_2 the amount of work required for compressors.

2.5. Microbial analysis

In order to evaluate the evolution of the population during the experiment, samples during the different stages were collected in sterile polypropylene tubes and immediately stored at −20 °C. Extraction of genomic DNA, polymerase chain reaction (PCR) amplification and denaturing gradient gel electrophopresis (DGGE) analysis were performed. The protocol described in the Fast® DNA Spin Kit for Soil (MP Biomedicals, LLC) handbook was used to extract DNA. The V6–V8 region of the bacterial 16S rRNA genes was amplified by PCR using the universal bacterial primers 968-F-GC and 1401-R (Sigma-Aldrich, St. Louis, MO, USA). The DGGE analysis of the amplicons was performed with a D-Code Universal Mutation Detection System (Bio Rad Laboratories) using 8%(w/v) polyacrylamide gels with a urea/formamide denaturing gradient of 45 to 65%. DGGE running conditions were applied according to Roest et al. (2005). The gels were stained with GelRed Nucleic Acid Gel Stain (biotium) and the most relevant bands were excised from the DGGE gel in order to identify the microorganisms present in the samples. Using the GelCompar IITM software (Applied Maths BVBA, Sint-Martens-Latem, Belgium) DGGE profiles were compared. After image normalization, bands were defined for each sample using the bands search algorithm within the program. Similarity indices were calculated from the densitometric curves of the scanned DGGE profiles by using the Pearson product–moment correlation coefficient (Häne et al., 1993). The peak heights in these densitometric curves were also used to determine the Shannon–Wiener diversity index (H). This index reflects the relative number of DGGE bands (sample richness) and relative intensity of every band (evenness). It ranges from 1.5 to 3.5 (low and high species evenness and richness, respectively) according to McDonald (2003). The taxonomic position of the sequenced DGGE bands was obtained using the RDP classifier tool (50% confidence level) (Wang et al., 2007). The closest cultured and uncultured relatives to each band were obtained using the BLAST search tool at the NCBI (National Centre for Biotechnology Information) (Mc.Ginnis and Madden, 2004). Sequences were deposited in GenBank Data Library under accession numbers MG692444-MG692471 (*archaeas*) and MG692472-MG692496 (bacteria).

In addition, Fluorescence *in situ* hybridization (FISH) was performed. First of all, samples were centrifuged during 5 min and 10000 rpm at 4 °C removing the supernatant. Paraformaldehyde (4% w/v) was used to fix biomass samples (250 μL) during 3 h. Then, they were washed three times with phosphate-buffered saline (PBS). Aliquots of 10 μL of samples were deposited on the wells of gelatin-coated, acid-washed, glass microscope slides and dehydrated by passing through a 50%, 80% and 100% (v/v) ethanol series. Hybridization with formamide (30% v/v) and the oligonucleotide probes was at 46 °C for 2 h. The following probes were used: EUB338 I (for most of bacteria, 5′-GCTGCCTCCCGTAGGAGT-3′), EUB338 plus (for Planctomycetales and Verrucomicrobiales, 5′-GCWGCCACCCGTAGGTGT-3′) and ARCH915 (for most of *archaea*, 5′-GTGCTCCCCCGCCAATTCCT-3′) (Daims et al., 1999). After hybridization step, and once the slides were washed and dried, the specimens were counter-stained for 5 min at room temperature with the DNA stain DAPI to quantify the total number of cells. 28 images were randomly acquired from inside each well on the slides using a Leica DM4000B microscope (Leica Microsystems, Wetzlar, Germany) for quantitative FISH analysis. *Archaea* appear red due to hybridization with the ARCH915 probe (red) while bacteria appear green due to hybridization with the EUB338 I and EUB338 plus probes (green) and DAPI (cyan). DAIME software was used to calculate the relative biovolumes of total *archaea* and total bacteria from the total DAPI-stained biomass. They were split into individual colour channels before image segmentation (Daims et al. 2006).

3. Results and discussion

3.1. Conversion of H_2 and CO_2 to CH_4

Biomass adaptation to the substrate took place during the set-up period when the feed mass flow rate of H_2 gas ($m_{H_2,\ IN}$) was 25.2 g/d (LR of 5.0 $m^3\ H_2/m^3_{reactor}$ d) and Q_R 8.0 L/min. A large part of the H_2 fed in these first days was transferred to the liquid phase and consumed but was not employed for CH_4 production, probably due to biomass adaptation to the substrate. Then, first stage started with a $m_{H2,IN}$ of 49.9 g/d (Fig. 3) and the same Q_R than set-up period. The mass balance performed to the gas phase showed that the average efficiency of H_2 utilization (η_{H2}) was 95% and an average methane yield (Y_{CH4}) of 0.18 $m^3\ CH_4/m^3\ H_2$ was observed. Average mass flow rate of H_2 transferred from gas to liquid phase ($m_{H2,\ G \rightarrow L}$) obtained was 44.6 g/d and an effluent mass flow rate of CH_4 gas as equivalent H_2 ($(m_{CH4,\ OUT})_{H2eq}$) according to Eq. (1) in average of 35.0 g/d. On day 26 $m_{H2,IN}$ was raised to 99.9 g/d (Fig. 3) while Q_R was maintained at 8.0 L/min (stage 2a). The increase in the mass flow rate provoked a slightly decrease in average η_{H2} until 85.7% thus indicating that mass transfer conditions were still acceptable even when the LR was doubled. However, the average Y_{CH4} obtained was slightly higher than in the previous stage, 0.19 $m^3\ CH_4/m^3H_2$. The difference between $m_{H2,\ G \rightarrow L}$ and $(m_{CH4,\ OUT})_{H2eq}$ was almost exactly the same in stage 1 and 2a and the values obtained were 82.2 g/d and 72.5 g/d respectively (Fig. 3). Biogas recirculation rate was increased to 12.3 L/min with the purpose of raising η_{H2} and the stage 2b started. Under this conditions, the performance of the MBR improve significantly, reaching an average η_{H2} value of 95% and Y_{CH4} reached of 0.21 $m^3\ CH_4/m^3\ H_2$, the highest obtained up to then. In this case, $m_{H2,\ G \rightarrow L}$ observed was 89.2 g/d and 80.1 g/d of (m

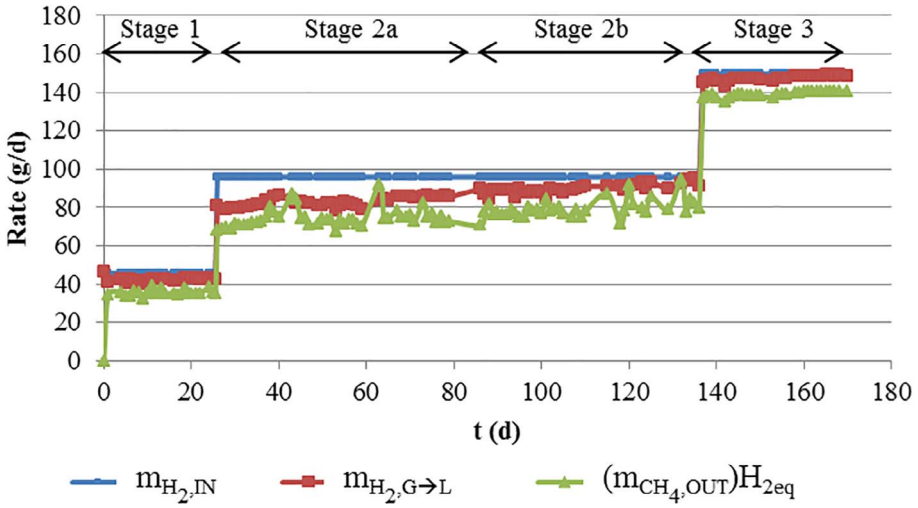

Fig. 3. Bioconversion performance during the experiment.

Table 2
Average k_La obtained in the different stages during the experiment of H_2 and CO_2.

	Stage 1	Stage 2		Stage 3
		2a	2b	
k_La_{H2} (h^{-1})	77	87	166	268
k_La_{CO2} (h^{-1})	54	61	117	190

Table 3
Maximum average specific utilization rate (U), average fraction of H_2 employed for methanogen growth (f_x), average Total Suspendid Solids (TSS) and average Volatile Suspended Solids (VSS) in the different stages during the experiment.

	Stage 1	Stage 2		Stage 3
		2a	2b	
U (g_{COD}/g_{VSS}·d)	6.0	7.7	4.7	3.53
f_x	0.22	0.12	0.11	0.09
TSS (g/L)	0.73	2.0	1.01	1.13
VSS (g/L)	0.44	1.6	0.91	1.02

$_{CH4,\ OUT})_{H2eq}$. The difference between them was in the same order of magnitude than the others (Fig. 3). This values were somewhat higher than the ones obtained in stage 2a, thus indicating that recirculation improved the amount of H_2 transferred from gas to liquid phase and the amount of CH_4 produced. Due to the high Q_R used in this stage, some foaming appeared in the reactor. This foaming disappeared naturally (without the use of antifoaming agents) after some weeks of the increase in the Q_R. At this point, $m_{H2,IN}$ was augmented to 149.8 g/d in combination with a maintained Q_R of 12.3 L/min (stage 3). During this stage, η_{H2} was 95% in average while Y_{CH4} increased until 0.22 m^3CH_4/m^3H_2, much closer to the maximum stoichiometric value of 0.25 m^3CH_4/m^3H_2. The same methane yield was obtained previously on a similar pilot-scale bioreactor (Díaz et al., 2015). The difference between $m_{H2,\ G\rightarrow L}$ and $(m_{\ CH4,\ OUT})_{H2eq}$ was lower than in previous stages meaning that *archaeas* employed almost all H_2 transferred to produce CH_4 (Fig. 3).

The MBR successfully transformed at least 95% of the H_2 fed at LR between 10 and 30 $m^3H_2/m^3_{reactor}$ d adjusting the gas recirculation rate. This highest LR is similar than that achieved on a similar pilot-scale bioreactor (40 $m^3H_2/m^3_{reactor}$ d in Díaz et al., 2015) with a hollow fiber membrane module and higher than those found in packed column bioreactors (4.5 $m^3H_2/m^3_{reactor}$ d) (Burkhardt and Busch, 2013) or CSTR (18 $m^3H_2/m^3_{reactor}$ d) (Kim et al., 2013). Therefore, this membrane module can be employed to transfer H_2 at a high rate, allowing the biological conversion to take place satisfactorily in a long-term which is a challenge to polymeric MBRs because of the operating problems related with the damage on account of thermophilic conditions in the polymeric materials.

3.2. MBR mass transfer capacity

The average k_La_{H2} values observed during the different stages in the experiment for the total gas flow thorough the membrane and the estimated k_La_{CO2} values are shown in Table 2. It should be draw attention to the fact that this maximum k_La_{H2} value is similar than those found in bioreactors with traditional gas diffusers (at equivalent gas rates), within the range of CSTR with high agitation speeds as 700 rpm (Kreutzer et al., 2005) and higher than the k_La_{H2} value achieved on a similar pilot-scale bioreactor (Díaz et al., 2015) to the LR of 30 $m^3H_2/m^3_{reactor}$ d. In general, this is the result of the large sparging area of the membrane module employed, which produces a good gas-liquid mass transfer interfacial area. On the other side, between the two MBRs, this can be explained as a result of the higher pore of ceramic module (0.8 μm versus 0.4 μm of polymeric module) and higher recirculation rate to transfer H_2.

3.3. Biological activity

It is very important the fact that the adaptation of an unspecific anaerobic thermophilic sludge to H_2 and CO_2 was accomplished. As a result, a methanogenic *archaeas* population was developed, which was capable of the bioconversion of H_2 and CO_2 into bioCH_4. The methane yield of 0.22 m^3CH_4/m^3H_2 is larger than the yields achieved employing specific strains of *M. thermoautotrophicum* (Jee et al., 1988; Peillex et al., 1990: 0.19 and 0.18 m^3CH_4/m^3H_2 respectively) or *Methanococcus thermolithotrophicus* (Peillex et al., 1988) at high efficiency of H_2 utilization values. From an industrial point of view, it can be translated into lower acquisition costs of specific hydrogenotrophic methanogens because an unspecific anaerobic sludge could be used as inoculum. The maximum specific utilization rate (U) and the fraction of H_2 employed for methanogen growth (fraction of H_2 consumed but not transformed to CH_4, f_x) are shown in Table 3. The maximum average specific utilization rate obtained was 7.7 g_{COD}/g_{VSS} d within the range of typical design value suggested from methanogens growing on H_2 and CO_2 (Rittman, 2001). At equivalent gas rates, the specific utilization rate obtained with this ceramic membrane bioreactor was always higher than the U value obtained on a similar pilot-scale bioreactor (Díaz et al., 2015) with hollow-fiber module.

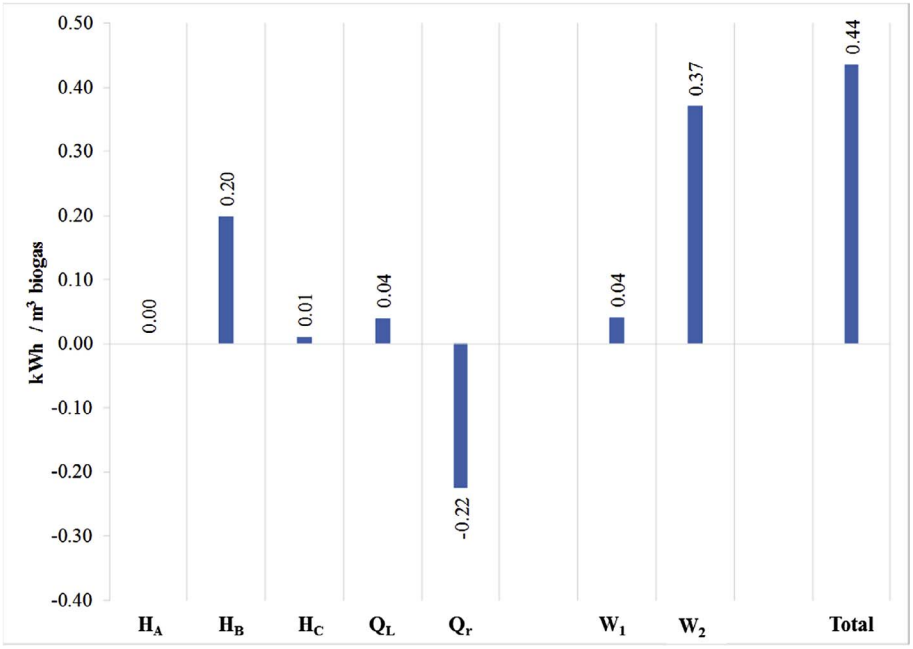

Fig. 4. Energy balance of the upgrading process. Energy rates are normalized by the rate of the upgraded biogas.

According to the results shown in Table 3, it could be stated that the highest value of f_x was obtained during the first stage. This fraction has dropped along the experiment, and in the last stage a decrease of more than 50% appeared. Then, this fraction was higher when mass flow rate of H_2 transferred from the gas to the liquid phase was low and vice versa thus indicating an uncoupling of microbial growth (anabolism) and H_2 conversion to CH_4 (catabolism). In addition, in the first stage of the experiments, the population of *archaeas* in the sludge was not likely to be plentiful as a result of the characteristics of conventional sewage sludge about microbial population and the limitation of this sludge in hydrolysis step. As was described in Díaz et al. (2015) previously, this fact took place because at the beginning of the experiment, especially in the set-up period, an important fraction of H_2 was utilized for microbial growth but when the sludge was completely adapted to the gas substrates, only a small fraction of H_2 was used for methanogen growth, almost all H_2 transferred was used to produce CH_4. At equivalent gas rates, the obtained f_x value with this ceramic MBR was always lower than the value obtained on a similar pilot-scale bioreactor (Díaz et al., 2015) with hollow-fiber membrane module.

VFA concentration was very low during the experiment: acetic acid concentration was under 100 mg/L and propionic acid was below 50 mg/L as it was in Díaz et al., 2015. pH was over the experiment between 6.8 and 7.9 and it was observed that the use of centrate as a nutrient solution helped to balance the pH.

The initial content of SST and SSV in the inoculum was 5.63 and 3.13 g/L respectively. After the set-up period, these values experienced a high decrease as a consecuence of the biomass adaptation to the new substrate. Average total and volatile suspended solids concentration analyzed during the experiment in the several stages of the experiment are shown in Table 3. These values showed an increasing trend from Stage 1 to Stage 2a. However, a decrease was produced in stage 2b when the recirculation rate was increase. This fact can be explained firstly, as a result of the high turbulence produced on account of the high recirculation rate employed and secondly, because of the appearance of foaming. This recirculation rate generated an obstacle to the growth of microorganisms being a breaking way for their and/or some losses of solids with the foaming. In the stage 3 of the experiment, it was observed an slightly increase in the content of VSS.

3.4. Consumption of energy

The total energy requirements for the upgrading process are 0.44 kWh per m^3 of biogas upgraded (Fig. 4). Energy consumption is dominated by the work required for gas recirculation (W_2 = 0.37 kWh/m^3 biogas), essential to transfer H_2 to the liquid phase at a high rate, while heat requirements (Q_{req}) are very low (0.025 kWh/m^3 biogas). These energy requirements are larger than those reported for the most used commercial technologies such as pressure-swing adsorption or water scrubbing (Bauer et al. 2013) in the range of 0.20–0.30kWh per m^3 of biogas. Nonetheless, it should be noted that 0.35 m^3 of new CH_4 can be formed per m^3 of biogas supplied to the system according to the maximum methane yield observed (0.22 m^3 CH_4/m^3 H_2). Since the enthalpy of combustion of CH_4 is 9.95 kWh/Nm^3 (802 kJ/mol), the equivalent energy stored in new CH_4 would be 3.5 kWh per m^3 of biogas upgraded. Therefore, the total energy requirements represent approximately 13% of the energy that could be obtained from the combustion of new CH_4 formed, hence the energetic benefit of the hydrogenotrophic upgrading process.

From a different angle, the potential energy stored as CH_4 increases from ~6 kWh per m^3, in the standard biogas plant (without upgrading) to ~9.5 kWh per m^3after the upgrading process. When discounted the total energy requirements of the upgrading process (0.44 kWh per m^3 of biogas), it can be observed an increase of ~50% in potential energy generation from CH_4. In this context, it is always worth mentioning that water electrolysis to produce H_2 for the upgrading process requires 7.2 kWh per m^3 of biogas, hence employing excess electricity production from wind and solar power, when they are in surplus, is a must in order that hydrogenotrophic upgrading can be applied. During these seasonal surpluses, the H_2 and CO_2 bioconversion processes, such as the studied, will be energetically beneficiaries.

Total energy consumption is slightly higher than the equivalent calculated for hollow-fiber membrane modules (Díaz et al., 2015), 0.3 kWh per m^3 of biogas, as a result of the higher pressure drop within the ceramic module. Conversely, ceramic membranes are more resistant, long-lasting and easy cleaned than polymeric though its high economic cost. Additionally, ceramic membrane modules can withstand higher rates than hollow-fiber modules because a higher pressure can be applied for gas sparging.

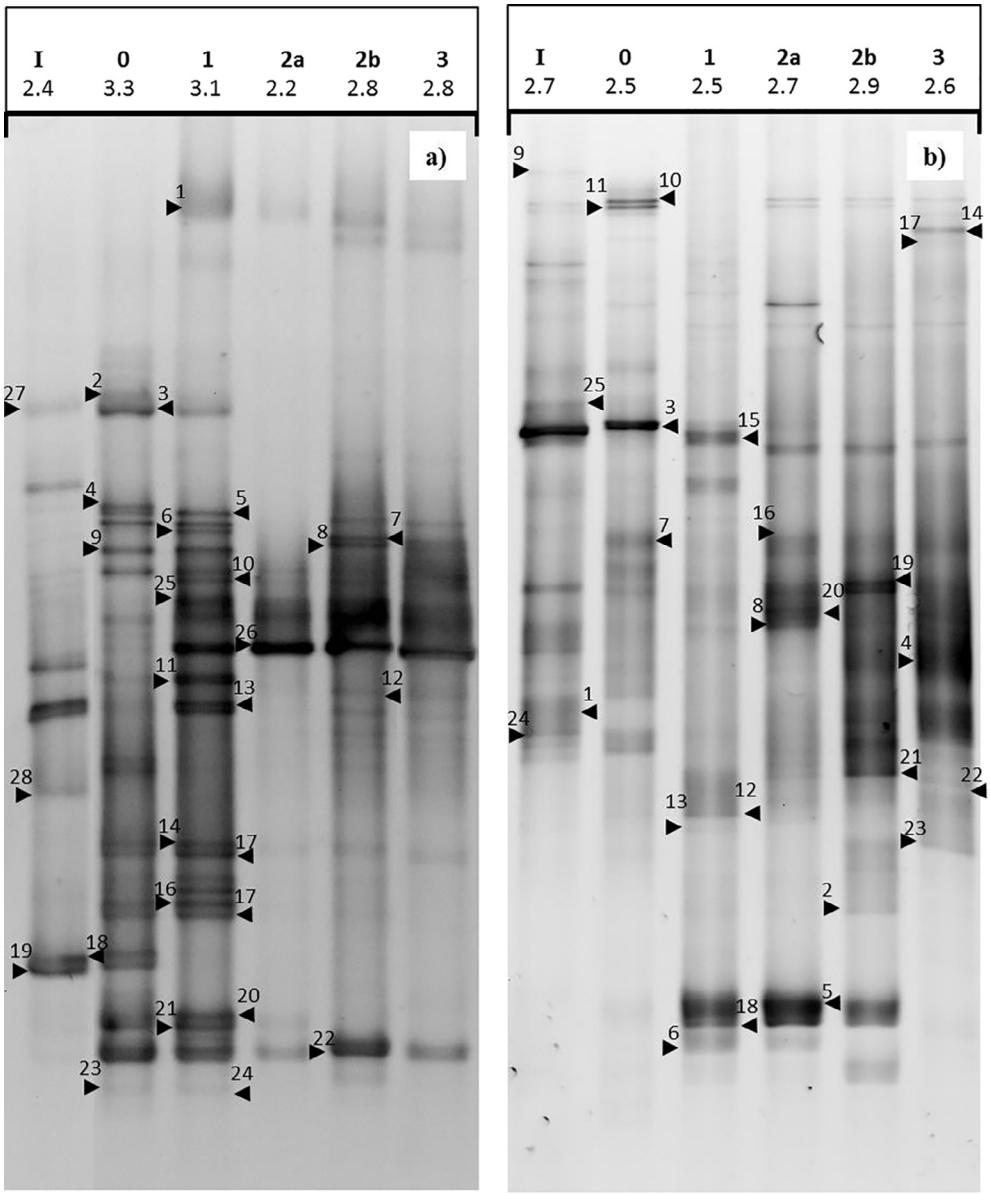

Fig. 5. a) Archaeal DGGE profiles and b) Bacterial DGGE profiles of the 16S rRNA amplicons of the samples with their respective diversity indices. Samples: Inoculum (I), set-up period (0) and stages 1–3 (1, 2a, 2b and 3).

Table 4
The abundances of archaea and bacteria related to the total biomass and ratio archaea/bacteria, in percentages. Samples: Inoculum (I), set-up period (0) and stages 1–3 (1, 2a, 2b and 3).

Sample	Archaea content (%)	Bacteria content (%)	Archaea/bacteria (%)
I	25.86	24.47	51.37
0	1.76	0.015	99.15
1	11.14	0.07	99.37
2a	22.29	0.035	99.84
2b	9.03	0.00	100.00
3	10.70	0.02	99.86

3.5. Microbial community

From the archaeal DGGE gel (Fig. 5a), twenty-eight bands were sequenced. According to the RDP classifier (confidence threshold of 50%), all of them belonged to the *Euryarchaeota* phyla and they were ascribed to two classes, almost all to *Methanobacteria* (band 1–27) and only one band to *Methanomicrobia* (band 28). The BLAST search tool provided consistent results with those given by the RDP classifier. *Methanothermobacter*, *Methanobacterium* and *Methanobrevibacter* were the three genus assigned to *Methanobacteria* class and *Methanosarcina* genus to *Methanomicrobia* class. After the biomass adaptation to the substrate during the set-up period, some new *archaeas* appeared and were present since then: band 14, 22 and 26 corresponding with three uncultered archaeon (KJ209721 and KF630660) with an identity of 100% and 99% respectively. Other new appeared achaeas (bands 2, 5, 9, 11, 15, 17, 20 and 24) were present only in some stages but not in all of them. However, as a result of the set-up period, some *archaeas* disappeared but later they appeared again and were present during the different stages of the experiment (band 6, 10, 25 and 28) and other disappeared completely (band 27). As is showed in Fig. 5a, *Methanothermobacter thermautotrophicus* was the *archaea* found with high level of similarity in all the stages of the experiment after the initial acclimation to H_2 and CO_2. This *archaea* was used previously in pure culture studies as in Peillex et al. (1990).

From the bacterial DGGE gel (Fig. 5b) and according to the RDP classifier (confidence threshold of 50%), twenty-five bands belonging to

three different phyla were sequenced: *Firmicutes* (band 1–18), *Proteobacteria* (band 19–23) and *Actinobacteria* (band 24) while one band remained unclassified (band 25). In general, the BLAST search tool provided consistent results with those given by the RDP classifier. *Firmicutes* was the predominant phylum with seven different genera. Two genera were assigned to *Proteobacteria* phylum and unclassified bacteria to *Actinobacteria* phylum. After the biomass adaptation to the substrate during the set-up period, some new bacteria appeared and were present during the whole experiment (band 7, uncultured bacterium JF417907), others disappeared but they were founded again in other stages (band 1, 8 and 16, all of them uncultured bacterium) and other ones were maintained (bands 4, 10 and 11). From the *Proteobacteria* Phylum, the Blast search tool assigned the DGGE band 21 to the genus *Tepidiphilus* with an identity of 100%, which was appeared after the set-up period and maintained during the different stages of the experiment. Although *Tepidiphilus thermophilus* could be a potential homoacetogen, acetoclastic methanogens (*Methanosarcina*) were not present in most of experiment stages and there was no VFA accumulation. Therefore, hydrogenotrophic pathway seems to be the main one to methane production.

A moderately high *archaea* richness and evenness was found with Shannon-Wiener diversity index range between 2,2 and 3,3 having the maximum value after the set-up period of the experiment (Fig. 5a). The diversity index calculated from the bacterial DGGE gel were in the range of 2,5 to 2,9 showing a moderate bacterial richness and evenness (Fig. 5b). The samples presented lower similarity index of *archaeas* during the experiment in comparison with the inoculum (similarity index values between 12.5 and 27.3), which can be linked with the development of a hydrogenotrophic community from a conventional thermophilic sludge with the new substrates (H_2 and CO_2). After the set-up period and during the different stages with several LR the similarity index was not so different (61.7–69.6) even when the recirculation rate was increased in stage 2b.

Archaea and bacteria were detected by FISH in all samples tested (Table 4). In the inoculum, *archaea* accounted for 25.86% of the microbial population, while bacteria represented 24.47% with ratio *archaea*/bacteria of 51.37%. After the set-up period, both *archaea* and bacteria content experienced a high decrease (being almost 0 the % of bacteria content) which can be linked with the decrease in the SSV above mentioned. Although the *archaea* content decreased in this period, the ratio *archaea*/bacteria was 99.15 joining with the acclimation process of the biomass previously explained to the new substrates (H_2 and CO_2) and the development of a methanogenic *archaeas* population. When the LR was augmented to 10 $m^3H_2/m^3_{reactor}$ d (stage 1) took place an increase in the content of *archaea* in comparison with the previous stage (more than 6 times). When this LR was doubled (stage 2a) the *archaea* content was doubled too. However, when an increased in the recirculation rate was performed (stage 2b) with the purpose of raising the efficiency of H_2 utilization, the content of *archaea* decreased (9.03%). This could be explain as a result of the previously mentioned high turbulence produced on account of the high recirculation rate employed which could be an obstacle to the growth of microorganisms or a breaking way for their. The content of *archaea* experienced a slightly increase in stage 3. All this results are in agreement with the SSV results showed previously. Otherwise, bacteria content had no significative changes since the set-up period. As is showed in Table 4, after the acclimation biomass period, *archaea* were predominant against bacteria.

4. Conclusions

The bioconversion of H_2 and CO_2 into bioCH_4 was feasible using an unspecific anaerobic thermophilic sludge as an inoculum after an adaptation period. The maximum loading rate of 30 $m^3 H_2/m^3_{reactor}$ d had a 95% efficiency in H_2 utilization and a methane yield of 0.22 $m^3 CH_4/m^3 H_2$. Gas sparging through the ceramic MBR showed a high capacity of H_2 mass transfer. k_La value of 268 h^{-1} was reached at 30 $m^3H_2/m^3_{reactor}$ d. *Methanothermobacter thermautotrophicus* was the *archaea* found with high level of similarity in all the experiment stages after the initial acclimation to H_2 and CO_2.

Acknowledgments

This research was supported by the Spanish Ministry of Education, Culture and Sports (FPU13/04680 Grant) and the funding company FCC-Aqualia in the project Smart Green Gas. The authors also thank the researchers Elisa Rodríguez, Patricia Ayala and Rebeca Pérez.

Appendix A. Supplementary data

Supplementary data associated with this article can be found, in the online version, at https://doi.org/10.1016/j.biortech.2018.02.087.

References

Angelidaki, I., Sanders, W., 2004. Assessment of the anaerobic biodegradability of macropollutants. Rev. Environ. Sci. BioTechnol. 3, 117–129.
APHA, AWWA, WPCF, 2005. Standard Methods for the Examination of Water and Wastewater, 21st ed., Washington, DC.
Atech Innovations, 2014. http://www.atech-innovations.com/fileadmin/downloads/Instructions_e_2014.pdf Accessed January 2016.
Bassani, I., Kougias, P.G., Treu, L., Angelidaki, I., 2015. Biogas upgrading via hydrogenotrophic methanogenesis in two-stage continuous stirred tank reactors at mesophilic and thermophilic conditions. Environ. Sci. Technol. 49 (20), 12585–12593.
Bassani, I., Kougias, P.G., Angelidaki, I., 2016. In-situ biogas upgrading in thermophilic granular UASB reactor: key factors affecting the hydrogen mass transfer rate. Bioresour. Technol. 221, 485–491.
Bassani, I., Kougias, P.G., Treu, L., Porté, H., Campanaro, S., Angelidaki, I., 2017. Optimization of hydrogen dispersion in thermophilic up-flow reactors for ex-situ biogas upgrading. Bioresour. Technol. 234, 310–319.
Bauer, F., Hulteberg, C., Persson, T., Tamm, D., 2013. Biogas upgrading – review of commercial technologies (Biogasuppgradering – Granskning av kommersiella tekniker). Report from the Swedish Gas Technology Center, Malmö.
Burkhardt, M., Busch, G., 2013. Methanation of hydrogen and carbon dioxide. Appl. Energy 111, 74–79.
Cruz, I., 2008. Energy storage technologies. Technical Business Conference. Department of eolic power. CIEMAT. Spain.
Daims, H., Brühl, A., Amann, R., Schleifer, K.H., Wagner, M., 1999. The domain-specific probe EUB338 is insufficient for the detection of all Bacteria: development and evaluation of a more comprehensive probe set. Syst. Appl. Microbiol. 22 (3), 434–444.
Daims, H., Lücker, S., Wagner, M., 2006. Daime, a novel image analysis program for microbial ecology and biofilm research. Environ. Microbiol. 8, 200–213.
Deng, L., Hägg, M.B., 2010. Techno-economic evaluation of biogas upgrading process using CO_2 facilitated transport membrane. Int. J. Greenhouse Gas Control. 4, 638–646.
Deublein, D., Steinhauser, A., 2011. Biogas from Waste and Renewable Resources: An introduction. Wiley.
Díaz, I., Lopes, A.C., Pérez, S.I., Fdz-Polanco, M., 2010. Performance evaluation of oxygen, air and nitrate for the microaerobic removal of hydrogen sulphide in biogas from sludge digestion. Bioresour. Technol. 101, 7724–7730.
Díaz, I., Pérez, C., Alfaro, N., Fdz-Polanco, F., 2015. A feasibility study on the bioconversion of CO_2 and H_2 to biomethane by gas sparging through polymeric membranes. Bioresour. Technol. 185, 246–253.
EurObservER, L'Observatoire des energies renouvelables, 2013. The state of renewable energies in Europe. ISSN 2101–9622.
EurObserver,, 2014. Biogas barometer. Accessed October 2015. http://www.eurobserver.org/biogas-barometer-2014/.
Granovskii, M., Dincer, I., Rosen, M.A., 2006. Economic and environmental comparison of conventional, hybrid, electric and hydrogen fuel cell vehicles. J. Power Source 159, 1186–1193.
Häne, B.G., Jäger, K., Drexler, H.G., 1993. The Pearson product-moment correlation coefficient is better suited for identification of DNA fingerprint profiles than band matching algorithms. Electrophoresis 14, 967–972.
Jee, H.S., Nishio, N., Nagai, S., 1988. Continuous CH_4 production from H_2 and CO_2 by Methanobacterium thermoautotrophicum in a fixed-bed reactor. J. Ferment. Technol. 66, 235–238.
Ju, D., Shin, J., Lee, H., Kong, S., 2008. Effects of pH conditions on the biological conversion of carbon dioxide to methane in a hollow-fiber membrane biofilm reactor (Hf – MBfR). Desalination 234, 409–415.
Kim, S., Choi, K., Chung, J., 2013. Reduction in carbon dioxide and production of methane by biological reaction in the electronics industry. Int. J. Hydrogen Energy 38, 3488–3496.
Kougias, P.G., Treu, L., Peñailillo Benavente, D., Boe, K., Campanaro, S., Angelidaki, I., 2017. Ex-situ biogas upgrading and enhancement in different reactor systems. Bioresour. Technol. 225, 429–437.

Kreutzer, M.T., Kapteijn, F., Moulijn, J.A., Ebrahimi, S., Kleerebezem, R., Van Loosdrecht, M.C.M., 2005. Monoliths as biocatalytic reactors: smart gas–liquid contacting for process intensification. Ind. Eng. Chem. Res. 44 (25), 9646–9652.

Lee, J.C., Kim, J.H., Chang, W.S., Pak, D., 2012. Biological conversion of CO_2 to CH_4 using hydrogenotrophic methanogen in a fixed bed reactor. J. Chem. Technol. Biotechnol. 87, 844–847.

Levene, J.I., Mann, M.K., Margolis, R.M., Milbrandt, A., 2007. An analysis of hydrogen production from renewable electricity sources. Sol. Energy 81, 773–780.

Luo, G., Angelidaki, I., 2012. Integrated biogas upgrading and hydrogen utilization in an anaerobic reactor containing enriched hydrogenotrophic methanogenic culture. Biotechnol. Bioeng. 109, 729–2736.

Luo, G., Angelidaki, I., 2013. Co-digestion of manure and whey for in situ biogas upgrading by the addition of H_2: process performance and microbial insights. Appl. Microbiol. Biotechnol. 97, 1373–1381.

Luo, G., Johansson, S., Boe, K., Xie, L., Zhou, Q., Angelidaki, I., 2012. Simultaneous hydrogen utilization and in situ biogas upgrading in an anaerobic reactor. Biotechnol. Bioeng. 109, 1088–1094.

Madigan, M.T., Brock, T.D., 2009. Brock Biology of Microorganisms. Pearson/Benjamin Cummings, San Francisco, CA.

Mc.Donald, G., 2003. Biogeography: Introduction to Space, Time and Life. Wiley, New York.

Mc.Ginnis, S., Madden, T.L., 2004. BLAST: at the core of a powerful and diverse set of sequence analysis tools. Nucl. Acids Res. 32.

Ni, M., Leung, M., Sumathy, K., Leung, D., 2006. Potential of renewable hydrogen production for energy supply in Hong Kong. Int. J. Hydrogen Energy. 31 (10), 1401–1412.

Peillex, J., Fardeau, M., Boussand, R., Navarro, J., Belaich, J.P., 1988. Growth of Methanococcus thermolithotrophicus in batch and continuous culture on H_2 and CO_2: influence of agitation. Appl. Microbiol. Biotechnol. 29, 560–564.

Peillex, J.P., Fardeau, M.L., Belaich, J.P., 1990. Growth of Methanobacterium thermoautotrophicum on H_2 & CO_2: High CH_4 productivities in continuous culture. Biomass 21, 315–321.

Perry, R.H., Green, D.W., Maloney, J.O., 1999. Perry's Chemical Engineers' Handbook. McGraw-Hill CD-ROM Handbooks, 7th ed. McGraw-Hill.

Rittman, B., 2001. Environmental Biotechnology: Principles and Applications. McGraw Hill, New York.

Roest, K., Heilig, H.G., Smidt, H., de Vos, W.M., Stams, A.J.M., Akkermans, A.D.L., 2005. Community analysis of a full-scale anaerobic bioreactor treating paper mill wastewater. Syst. Appl. Microbiol. 28, 175–185.

Strevett, K.A., Vieth, R.F., Grasso, D., 1995. Chemo-autotrophic biogas purification for methane enrichment: mechanism and kinetics. Chem. Eng. J. Biochem. Eng. J. 58, 71–79.

Suez Water Technologies – GE, 2014. https://www.suezwatertechnologies.com/products/zeeweed-hollow-fiber-membranes Accessed January 2018.

Wang, Q., Garrity, G.M., Tiedje, J.M., Cole, J.R., 2007. Naïve Bayesian classifier for rapid assignment of rRNA sequences into the new bacterial taxonomy. Appl. Environ. Microbiol. 73, 5261–5267.

Wang, W., Xie, L., Luo, G., Zhou, Q., Angelidaki, I., 2013. Performance and microbial community analysis of the anaerobic reactor with coke oven gas biomethanation and in situ biogas upgrading. Bioresour. Technol. 146, 234–239.